Microelectronic Engineering 122 (2014) 20–24

Contents lists available at ScienceDirect

Microelectronic Engineering

journal homepage: www.elsevier.com/locate/mee

A metal-embedded photo-mask for contact photolithography with application on patterned sapphire substrate

Jhih-Nan Yan [a], Cho-Wei Chang [a,b], Yung-Chun Lee [a,b,*]

[a] Department of Nanotechnology and Microsystems Engineering, National Cheng Kung University, Tainan 70101, Taiwan, ROC
[b] Department of Mechanical Engineering, National Cheng Kung University, Tainan 70101, Taiwan, ROC

ARTICLE INFO

Article history:
Received 13 November 2013
Received in revised form 27 February 2014
Accepted 13 March 2014
Available online 22 March 2014

Keywords:
Metal-embedded photo-mask
Pattern sapphire substrates
Light-emitting diode
Contact photolithography
Cone-shaped microstructure

ABSTRACT

This paper describes the fabrication processes of a new type of photo-masks, named metal-embedded photo-masks, which can be used in standard contact-type photolithography. This metal-embedded photo-mask is prepared by metal contact printing method and can easily achieve a line-width at sub-micrometer scales. The fabrication processes can be easily implemented and the cost of making a high-resolution photo-mask is significantly reduced. Both 2″ and 4″ quartz photo-masks with a line-width of 1 μm and 0.5 μm are successfully fabricated. Experimental patterning of photo-resist layers using these metal-embedded photo-masks are carried out. Applications of these photo-masks on fabricating high-quality patterned sapphire substrates (PSSs) used in light-emitting diode (LED) industry are experimentally demonstrated.

© 2014 Elsevier B.V. All rights reserved.

1. Introduction

Fabrication of micro/nano-structures has been an active topic in research and plays an important role in the development of modern sciences and technologies. Many methods have been successfully developed in the past few decades for fabricating small structures at micro- and/or nano-scales [1–3]. The most dominant and successful method is photolithography, which has been widely used in semi-conductor industry as well as other applications [4–6]. There are three types of photolithography, namely contact, proximity, and projection photolithography. All three types of photolithography require a photo-mask to transfer a designed pattern to a photo-resist (PR) layer deposited on a substrate through ultraviolet (UV) exposure [7]. Conventional photo-masks are made by patterning a metal (mostly chrome, Cr) film on top of a glass or fused quartz plate. In contact and proximity photolithography, the photo-mask is either in direct contact or in close proximity to the PR/substrate [8]. Parallel UV light with uniformly distributed intensity passes through the photo-mask to transfer the image of photo-mask directly to the PR layer. The strength of contact or proximity photolithography lies in its simplicity and easiness in implementation, as well as its high throughput for large-area patterning. However, the photo-masks are easily subjected to PR contamination and contact wear damage and hence are with limited lifetime. Furthermore, to obtain a photo-mask with a line-width below 1 μm can be very expensive because it may require using an electron-beam lithography system [9–12]. On the other hand, projection type of photolithography patterns the PR layer through a de-magnified optical image projection system. Smaller line-width is achieved and the photo-mask is less vulnerable. However, projection type photolithography requires a high-quality optical imaging system and a precision stepping mechanism [13,14]. The capital investment and running cost of projection photolithography are very high, which is a problem to both academia and industry.

This paper interests in contact and proximity types of photolithography. As mentioned above, several important but unsolved issues in contact and proximity photolithography are directly related to the manufacturing of photo-masks. For example, it is desirable to push the line-width down to sub-micrometer scale but at the same time without increasing the cost of mask fabrication. Another issue is how to reduce the chance of mask contamination or damage to prolong the lifetime of photo-mask. Furthermore, if the mask contamination and damage cannot be avoided and the photo-masks are treated as consumable parts, a simple and cost-effective method for manufacturing photo-masks with a given line-width become critically important for real industrial applications.

In this work we propose a new type of photo-mask named metal-embedded photo-mask for the applications in contact and proximity photolithography. This metal-embedded photo-mask can be easily and cost-effectively fabricated based on a metal

* Corresponding author at: Department of Mechanical Engineering, National Cheng Kung University, Tainan 70101, Taiwan, ROC. Tel.: +886 6 2757575x62101/62177; fax:+ 886 6 2094010.
E-mail address: yunglee@mail.ncku.edu.tw (Y.-C. Lee).

http://dx.doi.org/10.1016/j.mee.2014.03.008
0167-9317/© 2014 Elsevier B.V. All rights reserved.

contact printing photolithography proposed earlier by one of the authors [15–17]. Fig. 1 shows schematically the fabrication procedures of a metal-embedded photo-mask. It starts from a PDMS soft mold which can be replicated from a silicon mold by conventional casting and molding processes [18]. A metal film is thermally evaporated on the mold surface which may cover both the concave and convex surface areas of the PDMS mold. A quartz plate is used for making the photo-mask and a PR layer is spin-coated on the quartz surface, as shown in Fig. 1(a). In the second step as shown in Fig. 1(b), the metal-film coated PDMS mold is brought into contact with the PR-layer coated quartz substrate. After applying certain contact pressure and thermal heating, the PDMS mold is then separated from the quartz substrate and the patterned metal-film defined by the convex surface features of the PDMS mold will transfer to the PR layer deposited on the quartz substrate, as shown in Fig. 1(c). This is known as metal contact printing. After UV exposure and PR developing, as shown in Fig. 1(d) and (e), respectively, the quartz substrate is sent to a reactive ion etching (RIE) system. Surface microstructures are created on the quartz surface using the patterned metal film and PR layer as an etching mask, as shown in Fig. 1(f). A metal film is then deposited on top of the quartz substrate, as shown in Fig. 1(g), and finally a metal-embedded photo-mask is obtained after a lift-off process as shown in Fig. 1(h).

The metal-embedded photo-mask differs from conventional one in that the patterned metal film is embedded into the quartz plate. When applying to a contact photolithograph for example, both photo-masks can perform exactly the same function of UV exposure of a PR layer as shown in Fig. 2 [19]. As a matter of fact, the proposed metal-embedded photo-mask may have some advantages in comparison with a conventional one. For example, since the metal film is sitting on a withdrawing position from the top surface of photo-mask, it has less direct contact with the PR layer and is less vulnerable to PR contamination and wear damage. Furthermore, the UV light can directly pass through the quartz/PR interface without going through a thin air gap, which may have a higher light transmittance and less light diffraction effect. Perhaps the most important advantage is in the metal contact printing method for fabricating photo-masks. First of all, the line-width can easily go down to sub-micrometer scale or even smaller. Secondly, the equipments needed for carrying out this fabrication process are relatively common and readily available. Therefore the processes can be easily implemented and the cost of photo-mask fabrication is significantly cut down, which may partially solve the problem of mask contamination and damage from an economical point of view.

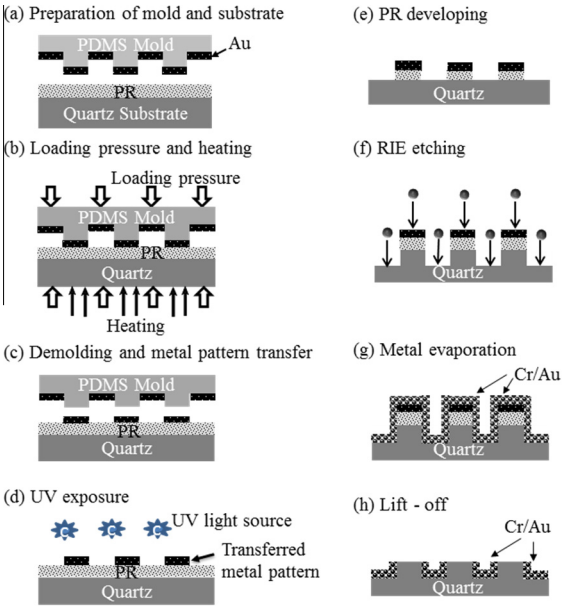

Fig. 1. A schematic diagram of the flow chart for fabricating a metal-embedded photo-mask.

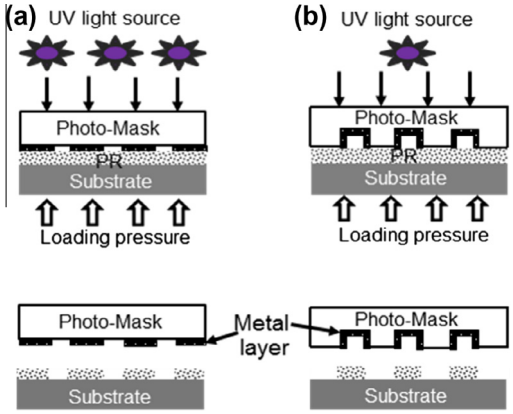

Fig. 2. UV exposure and PR developing using (a) a conventional contact photo-mask and (b) a metal-embedded photo-mask.

In this work, to demonstrate the potential of this new metal-embedded photo-mask and its fabrication process, the fabricated photo-mask will be used for the manufacturing of patterned sapphire substrates (PSSs) used in light-emitting diode (LED) industry [20]. A PSS is a sapphire substrate with patterned three-dimensional (3D) surface micro-structures which can enhance the light extraction efficiency of LEDs. The majority of PSSs are made by first photo-lithographically patterning a layer of PR micro-structures on the surface of a sapphire substrate, and then applying ion-coupled plasma (ICP) etching on the sapphire substrate. In this work, both 2″ and 4″ PSSs with a feature size down to 1 μm will be fabricated using the proposed metal-embedded photo-masks.

2. Experimental methods

2.1. Soft PDMS mold reproduced silicon mold process

In this work, we have prepared two silicon master molds (8″ wafers) with two different surface microstructures by standard photolithography from a local semiconductor company (DataWise Technology Company, Taiwan). One of the silicon molds has a hexagonal array of micro-pillars with a diameter of 1 μm, a center-to-center pitch of 2 μm, and a pillar height of 0.4 μm. Another silicon mold has a hexagonal array of micro-holes with a diameter of 0.5 μm, a center-to-center pitch of 1 μm, and a hole-depth of 0.4 μm. Since the PDMS mold is negatively replicated from the silicon mold, the nature of surface microstructures is reversed. Following the metal contact printing processes shown in Fig. 1, a PDMS mold with arrayed micro-holes will finally yield a metal-embedded photo-mask which contains arrayed micro-holes and the metal films are coated on the inner surfaces of holes. On the other hand, for a PDMS mold with arrayed micro-pillars, the fabricated photo-mask will contain arrayed micro-pillars and the metal film will cover all surfaces except for the top end surfaces of the micro-pillars.

2.2. Fabrication of metal-embedded photo-masks process

In preparing the PDMS mold, the PDMS (Sylgard 184, Dow Corning, USA) is cured at 90 °C for 1 h and then de-molded from the

silicon master mold. A 50 nm thick Au film is then deposited on the PDMS mold surface by an electron-beam thermal evaporator (VT1–10CE, ULVAC, Kanagawa, Japan) at a rate of 0.6 Å/s. For the quartz substrate, a positive tone photo-resist (AZ1500, AZ Electronic Materials, Japan) is spin-coated on the quartz substrate. The PR layer has a thickness of around 900 nm and is soft baked at 100 °C for 60 s. After the mold and the substrate are prepared, processes of metal contact printing as depicted in Fig. 1(b) and (c) are carried out. The intimate contact between the PDMS mold and quartz substrate is critically important and a uniform pressure of 2 MPa and a temperature of 95 °C for 2 min are applied in the process shown in Fig. 1(b). After the printing process, the PR layer is patterned with a 50 nm thick Au film which is transferred from the PDMS mold. The PR layer is then exposed to UV light while using the patterned metal film as a photo-mask. The exposure time is 1.4 s using a I-line (405 nm) UV source and an energy intensity of 22 mW/cm^2. After PR developing, a layer of patterned PR microstructures is formed on the quartz surface and is hard bake at 110 °C for 90 s. The transferred Au film and the patterned PR layer are then serving as an etching mask for subsequent RIE etching on the quartz substrate. The power of RIE (200RL-RIE, CORIAL, France) is set to 200 W, the pressure in the reaction chamber is 70 mTorr, and the flow rate of gas CF_4 and SF_6 are controlled at 50 and 40 sccm, respectively. A 50 nm thick Cr film and a 20 nm tick Au film are then deposited sequentially on the quartz substrate surface by the e-beam thermal evaporator at a rate of 1 and 0.6 Å/s, respectively. Finally we lifted off the PR layer and the metal layers on top of it by rinsing the sample in acetone, and a metal-embedded photo-mask is fabricated as shown in Fig. 1(h).

As mentioned above, we have prepared two different silicon molds: one has arrayed pillars with a features size of 1 μm and the other one has arrayed holes with a 0.5 μm feature size. Both silicon molds have been applied in the fabrication processes shown in Fig. 1 to produce their corresponding metal-embedded photo-masks. Fig. 3 shows the SEM images from both top and cross-section of the fabricated photo-mask when using the silicon mold containing arrayed pillars of 1 μm in diameter. This metal-embedded photo-mask has arrays of hexagonally micro-holes with a diameter of 1.2 μm and a center-to-center pitch of 2 μm, as shown in Fig. 3(a). As shown in Fig. 3(b), the bottom surface and side-wall of the hole are covered by a Cr/Au metal film as we expect from the fabrication processes. The difference between the 1.0 μm pillar diameter in the silicon mold and the 1.2 μm hole-diameter in quartz metal-embedded photo-mask is mostly come from side-etching effect in the RIE etching process depicted in Fig. 1(f). Some compensation in the design of silicon mold is needed if precision dimension in the photo-mask is required.

Using the other silicon mold which has arrayed holes with a hole-diameter of 0.5 μm, another metal-embedded photo-mask is successfully fabricated and its SEM images are shown in Fig. 4. As shown in Fig. 4(a), it has a hexagonal array of micro-pillars with a diameter of 435 nm and a center-to-center pitch of 0.5 μm. Again, the 435 nm pillar diameter in the photo-mask is less than the 500 nm hole-diameter in silicon mold because of the side-etching in RIE process. Also observed in Fig. 4(b) is that the surface of the quartz photo-mask is covered with a Cr/Au metal film except

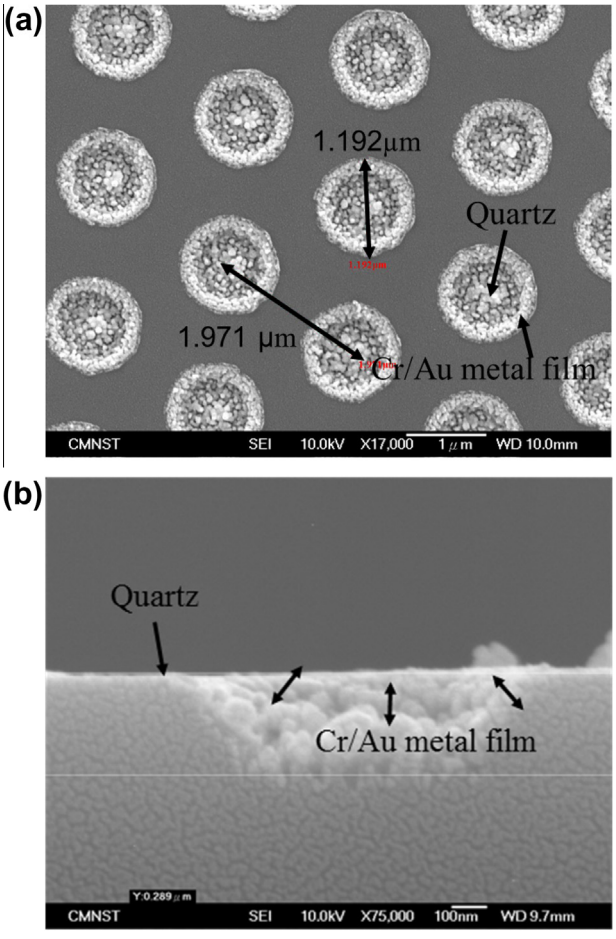

Fig. 3. SEM images of (a) the top view of a metal-embedded quartz photo-mask which contains hexagonal arrays of metal-deposited micro-holes with a diameter of 1.2 μm and a period of 2 μm, and (b) the cross-section view of the metal-deposited micro-holes.

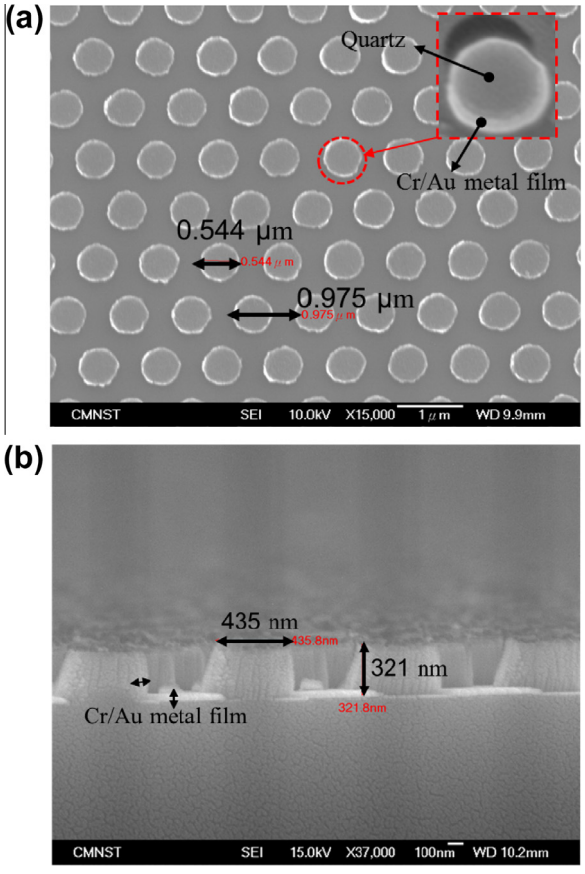

Fig. 4. SEM images of (a) the top view of a metal-embedded quartz photo-mask which contains hexagonal array of micro-pillars with a diameter of 435 nm and a period of 1 μm, and (b) the cross-section view of the metal-deposited on micro-pillars.

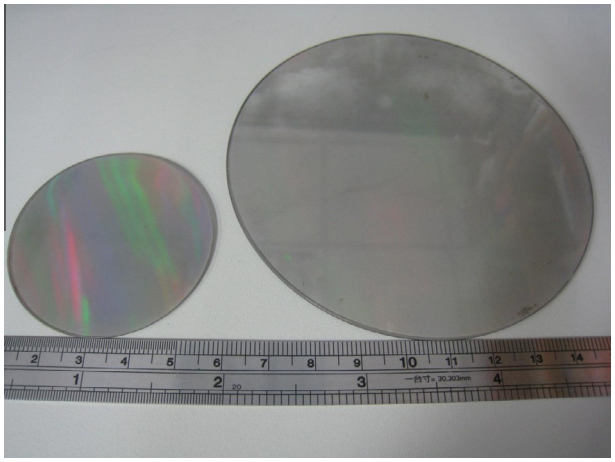

Fig. 5. A photo of a 2″ (left) and a 4″ (right) metal-embedded photo-masks which contain hexagonally arrays of micro-holes with a hole-diameter of 1.2 μm and a center-to-center pitch of 2 μm.

at the top end surface of these hexagonally arrayed micro-pillars, which provide a passage of UV light hen using this metal-embedded photo-mask in contact or proximity photolithography.

As shown in the photo of Fig. 5, both 2″ and 4″ quartz metal-embedded photo-masks are successfully fabricated and can be used for patterning PR layer. Photo-masks with larger dimensions are also possible if they are within the area size of the 8″ silicon mold and can be accommodated by all equipments involved in the fabricating processes.

3. Results and discussion

3.1. Photo-resist patterning for contact photolithography

The fabricated quartz photo-masks described in previous section are used in contact photolithography for patterning a PR layer on a substrate. The same photo-resist AZ1500 used in previous section is used here again. Since we are particularly interested in applying this new type of photo-masks for the fabrication of patterned sapphire substrates (PSSs) used in LED industry, the AZ1500 PR is coated on a sapphire substrate. The purpose of the PR layer, after photolithography patterning, is to act as an etching mask when applying ICP etching on the sapphire substrate. In order to achieve certain etching depth and profile control on the final 3D microstructures on sapphire surface, the PR layer thickness is important and is chosen to be a 1.3 μm. After the AZ1500 PR layer is spin-coated on a sapphire substrate, the metal-embedded photo-mask which contains arrayed holes with metals coated on their inner surfaces shown in Fig. 3 is used for contact photolithography. After standard UV exposure and PR developing process, patterned PR microstructures are successfully formed and their SEM images in both cross-section view and tilted view are shown in Fig. 6(a) and (b), respectively. As seen from Fig. 6, these hexagonally arrayed PR micro-pillars have a height of 1.3 μm, which match the original PR layer thickness, and a diameter of 1.0 μm, which is smaller than the 1.2 μm hole-diameter in the used photo-mask. The shrinkage in pillar's diameter is because we want to achieve a high aspect ratio of 1.3 for the PR microstructures so that the ICP etching on sapphire substrate can be successfully carried out. To achieve high aspect ratio in PR, the UV dosage and PR developing parameters are adjusted which results in a smaller pillar diameter.

To test the patterning resolution, the metal-embedded photo-mask which contains micro-pillars with a diameter of 435 nm as

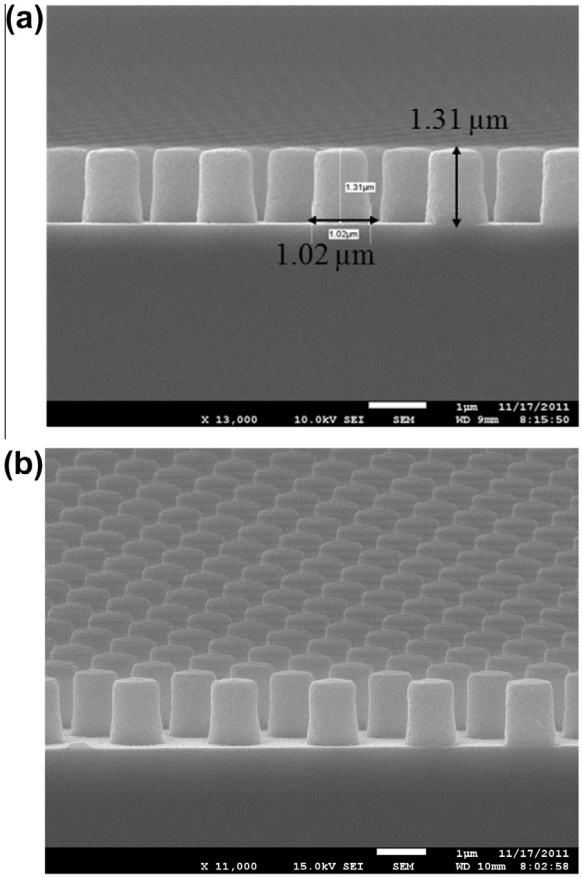

Fig. 6. (a) A cross-section view and (b) a tilted view SEM images of the developed PR microstructures on a sapphire substrate using a metal-embedded photo-mask; the hexagonal array of micro-pillars has a diameter around 1 μm and a height of 1.3 μm.

shown in Fig. 4 is also used in standard contact photolithography. The AZ1500 PR is spin-coated on a sapphire substrate and the PR layer thickness is around 200 nm. After UV exposure and PR developing, the SEM image of obtained PR microstructures is shown in Fig. 7. Since the UV light is passing through the top end surfaces of the micro-pillars of the photo-mask and the AZ1500 is a positive-tone PR, hexagonally arrayed micro-holes are formed on the PR layer after UV exposure and PR developing. The hole-diameter is around 370 nm and a depth of 190 nm which is approximately close to the pillar diameter in the photo-mask. It is understood that the dimensional accuracy in photolithography patterning at sub-micrometer scale is quite sensitive and subjected to a number of processing parameters. Nevertheless, it is demonstrated that patterning at sub-micrometer scales using this new type of metal-embedded photo-mask is possible and applicable.

3.2. Applications in PSS

Using the PR pillar arrays as an etching mask, the sapphire substrate is then subjected to dry etching by an ICP system (NE-550EX, ULVAC, Japan). In this dry etching process, the ICP power, RF bias power, BCl_3 flow rate and chamber pressure are kept at 900 W, 150 W, 40 sccm and 5 mTorr, respectively [20]. The ICP etching time is 20 min and the fabrication of PSSs is completed. Cone-shaped surface microstructures as shown in Fig. 8 are obtained on the sapphire surface. The diameter and the height of these conical microstructures are 1.4 μm and 1.1 μm, respectively, and the spacing between them is 0.4 μm. Fig. 9 shows the 2″ and 4″ pattern

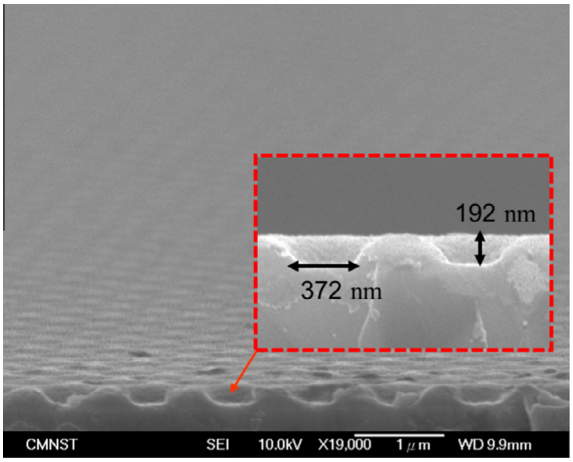

Fig. 7. SEM image of a hole-arrayed PR sub-micrometer structure with a hole diameter around 370 nm and a depth of 190 nm fabricated on sapphire substrate using a quartz metal-embedded photo-mask.

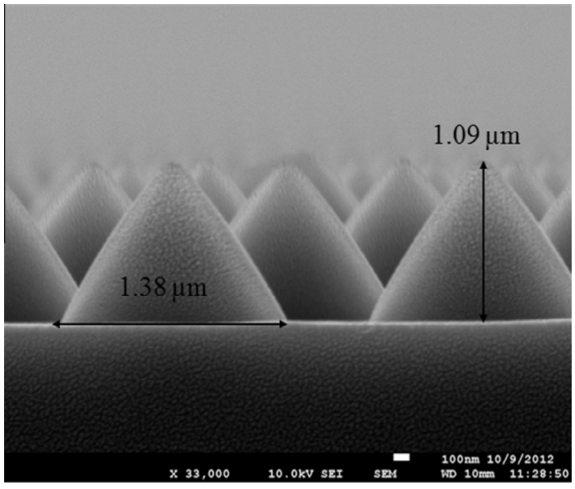

Fig. 8. The patterned sapphire substrate (PSS) with cone-shaped surface microstructures after ICP etching; the diameter/spacing/height are 1.4 μm/0.4 μm/1.1 μm, respectively.

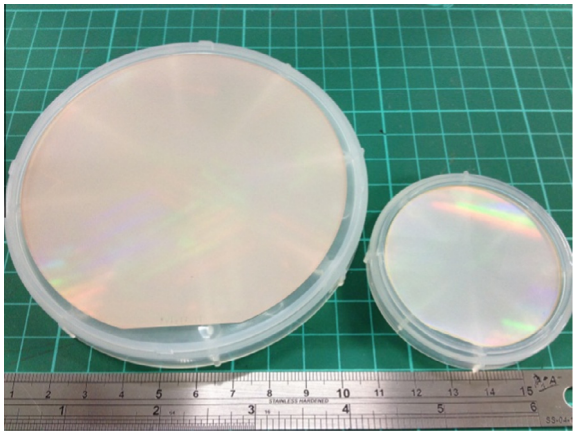

Fig. 9. A photo of a 4″-diameter PSS (left) and a 2″ PSS(right).

sapphire wafers which is fabricated by metal metal-embedded photo-mask process and contact photolithography method. These specifications meet the standard requirements in LED industry and the fabricated PSSs can be directly used for the manufacturing of high brightness LEDs.

4. Conclusion

In this paper, we demonstrate experimentally the fabrication processes of a new type of metal-embedded photo-mask which can be used in standard contact photolithography. In comparison with conventional photo-masks, the line-width of this new photo-mask can easily do down to sub-micrometer scales and possibly nanometer scale if the silicon mold is available. Such a small line-width is possible for conventional photo-masks but may require using e-beam lithography systems which are very expensive and at a low throughput. Furthermore, for this new type of photo-masks, the metal film is embedded inside the concave surface of the photo-mask and hence is less vulnerable to wearing damage or photo-resist contamination during contact photolithography. While for conventional photo-masks, the metal film is exposed outside and in contact with photo-resists or substrates and the lifetime of photo-masks is shorten due to possible damaged or contamination. Besides, the fabrication processes are relatively simple and easy for this new type of photo-masks, and hence can be implemented in most laboratories. The cost of making high-resolution photo-masks is therefore significantly cut down, which might be a way to solve the problem of photo-mask consumption in industrial applications of contact photolithography. As an example for demonstration, we have applied these metal-embedded photo-masks to the fabrication processes of PSSs. Both 2″ and 4″ PSSs with cone-shaped surface microstructures are successfully fabricated in laboratory.

Acknowledgments

This work was funded by the National Science Council (NSC) of Taiwan, Republic of China (ROC) under Grant NSC 101-2120-M-006-004-CC1.

References

[1] Y. Choi, S. Hong, L.P. Lee, Nano Lett. 9 (2009) 3726–3731.
[2] G. Li, Q. Dong, J. Xin, C.W. Leung, P.T. Lai, W.Y. Wong, P.W.T. Pong, Microelectron. Eng. 110 (2013) 192–197.
[3] C.W. Chang, C.Y. Chen, T.L. Chang, C.J. Ting, C.P. Wang, C.P. Chou, Appl. Phys. A 109 (2012) 441–448.
[4] J.W. Kim, U. Plachetka, C. Moormann, H. Kurz, Microelectron. Eng. 110 (2013) 403–407.
[5] Z. Cui, J. Du, Q. Huang, J. Su, Y. Guo, Microelectron. Eng. 53 (2000) 153–156.
[6] W. Zhou, J. Zhang, X. Li, Y. Liu, G. Min, Z. Song, J. Zhang, Appl. Surf. Sci. 255 (2009) 8012–8019.
[7] J.C. Love, D.B. Wolfe, H.O. Jacobs, G.M. Whitesides, Langmuir 17 (2001) 6005–6012.
[8] K.W. Kwon, J.C. Choi, K.Y. Suh, J. Doh, Langmuir 27 (2011) 3238–3243.
[9] Z. Jahed, S. Jin, M.J. Burek, T.Y. Tsui, Mater. Sci. Eng. A 542 (2012) 40–48.
[10] C.I. Chang, Y.L. Lai, C.P. Liu, R.C. Wang, J. Phys. Chem. Solids 69 (2008) 420–424.
[11] Y.K. Su, J.J. Chen, C.L. Lin, S.M. Chen, W.L. Li, C.C. Kao, J. Cryst. Growth 311 (2009) 2973–2976.
[12] H.W. Huang, H.C. Kuo, J.T. Chu, C.F. Lai, C.C. Kao, T.C. Lu, S.C. Wang, R.J. Tsai, C.C. Yu, C.F. Lin, Nanotechnology 17 (2006) 2998–3001.
[13] T.S. Kim, S.M. Kim, Y.H. Jang, G.Y. Jung, Appl. Phys. Lett. 91 (2007) 171114.
[14] J. Wang, L.W. Guo, H.Q. Jia, Z.G. Xing, Y. Wang, J.F. Yan, N.S. Yu, H. Chen, J.M. Zhou, J. Cryst. Growth 290 (2006) 398–404.
[15] Y.C. Lee, C.Y. Chiu, J. Micromech. Microeng. 18 (2008) 075013.
[16] J.A. Gardener, J.A. Golovchenko, Nanotechnology 23 (2012) 185302.
[17] A. Beduer, F. Seichepine, E. Flahaut, C. Vieu, Microelectron. Eng. 97 (2012) 301–305.
[18] A. David, Y. Chang, K. Eich, B.K. Gale, J. Lightwave Technol. 23 (2005) 2088–2093.
[19] Y.J. Lee, J.M. Hwang, T.C. Hsu, M.H. Hsieh, M.J. Jou, B.J. Lee, T.C. Lu, H.C. Kuo, S.C. Wang, IEEE Photonics Technol. Lett. 18 (2006) 1152–1154.
[20] W.F. Yang, Q.Z. Zhang, M.G. Wang, Y. Xia, Sci. China Technol. Sci. 54 (2011) 2232–2236.